

## Near-field effects in VSP-based Q-estimation for an inhomogeneous model

Arnim B. Haase and Robert R. Stewart

### ABSTRACT

As a continuation of earlier near-field investigations into homogeneous situations we expand our analysis to an inhomogeneous example. We show that depth locations of so-called *wrap-around* points where spectral ratio method Q-estimates change from large negative values to large positive values are controlled by P-wave velocities and intrinsic Q-factors. A velocity-step model and Q-factors derived from these velocities by empirical equation are used to demonstrate near-field Q-factor recovery by inversion. Because VSP model data and forward models are computed with the same multi-interface Sommerfeld integral it is found that, in this noise-free situation where velocities and densities are assumed to be known exactly for the forward modelling step, Q-factors can be recovered exactly also. Even though this VSP model approach is a simplification in many respects it does include near-fields, far-fields and geometrical spreading in the analysis.

### INTRODUCTION

The near-field of a seismic source can cause significant Q-estimation errors when the spectral ratio method is employed (Haase and Stewart, 2008). Figure 1 shows near-field log-magnitude spectra for the depth range from 15m to 61m computed with the Sommerfeld-integral (Figure 5 of the 2008 Report); note that relative amplitudes are retained by global scaling to zero dB. The parameters for this earth model are

$$V_p = 2000\text{m/s},$$

$$V_s = 879.88\text{m/s},$$

$$\rho = 2400\text{kg/m}^3 \text{ and}$$

$$Q_p = 100.$$

Figure 2 demonstrates what the spectral ratio method “*sees*” (Figure 6 of the 2008 Report); all spectra are equalized to their maximum amplitudes (zero dB scaling applied individually). The down going wave in Figure 2 *appears* to gain high frequency strength. This implies negative Q-factors. For completeness, far-field log-magnitude spectra with zero dB scaling applied individually are given in Figure 3 (Figure 12 of the 2008 Report). At 61m depth, and below, amplitudes decay with depth and frequency as expected by the spectral ratio method which implies positive Q-factors. A near-field region spectral ratio can be seen in Figure 4 (Figure 7 of the 2008 Report); frequency dependence of Q-estimates is evident. Figure 5 finally shows the depth dependence of spectral ratio method Q-estimates (Figure 9 of the 2008 Report); the near-field region is characterized by negative Q-factors and the model Q-factor of 100 is approached deeper into the far-field region independent of the estimation frequency range. Large Q-factors are caused by spectral ratios in the transition region between near-field and far-field where the log-

magnitude spectra in Figure 2 are almost parallel. Of particular interest is the *wrap-around* look at the depths where the quality factor Q changes polarity.

The results reviewed above are obtained for a homogeneous model. A more realistic inhomogeneous situation is investigated in this report.

### THE INHOMOGENEOUS NEAR-FIELD MODEL

A first indication of spectral ratio method Q-estimates in inhomogeneous media is given in Figure 6. This real-data heavy oil sand Q-estimation example (Ortiz-Osornio and Schmitt, 2008) appears to suffer from *wrap-around* effects similar to the constant velocity case of Figure 5. The depth scale of Figure 6 seems to confirm the expectation of near-field effects in this situation. Details of these measurements are not known but the presence of several *wrap-around* features suggests that *wrap-around* points can be repeated at increasing depths as velocities increase. What, then, is the velocity dependence of these *wrap-around* points? To answer this question the near-field spectral compensation introduced by Haase and Stewart (2008) is utilized. Normalizing by near-field multiplier magnitudes

$$M_{\text{near}} = \sqrt{1 + V_p^2 / (\omega z)^2} \quad (1)$$

leads to a modified spectral ratio which is a first order approximation:

$$\ln \left[ \frac{A(\omega)_{z+\Delta z} / \sqrt{1 + \left(\frac{V_p}{\omega(z+\Delta z)}\right)^2}}{A(\omega)_z / \sqrt{1 + \left(\frac{V_p}{\omega z}\right)^2}} \right] = -\frac{\omega}{2QV_p} \Delta z \quad (2)$$

Equation 1 shows that relative near-field strength is controlled by velocity, depth and frequency. Near-field strength is diminished by increasing frequency and increasing depth but an increase in velocity has the opposite effect by boosting it. At *wrap-around* points the slope in Equation 2 is zero because the amplitude ratio is independent of frequency; amplitude spectra can still be functions of frequency but their ratios are not at these depth locations. Assuming that, for *wrap-around* points, amplitude ratios are the same at different frequencies we derive from Equation 2

$$\Delta z \frac{(\omega_1 - \omega_2)}{2QV_p} + \frac{1}{2} \ln \left[ \frac{1 + \left(\frac{V_p}{\omega_1 z}\right)^2}{1 + \left(\frac{V_p}{\omega_1(z + \Delta z)}\right)^2} \frac{1 + \left(\frac{V_p}{\omega_2(z + \Delta z)}\right)^2}{1 + \left(\frac{V_p}{\omega_2 z}\right)^2} \right] = 0 \quad (3)$$

When  $V_p$ ,  $Q$ ,  $\Delta z$ ,  $\omega_1$  and  $\omega_2$  are given, trial solutions for a range of depth values  $z$  can be computed from Equation 3; the approximate *wrap-around* location in depth is indicated by the trial solution zero-crossing. Repeating these computations for a range of velocities and Q-factors leads to the curves given in Figure 7. We see that *wrap-around* point locations are shifted to larger depths with increasing velocities and increasing Q-factors in homogeneous situations. On inspection of the near-field multiplier given in Equation 1 this velocity dependence makes intuitive sense.

Next we investigate the velocity step model shown in Figure 8. Velocities are seen to increase in the near-surface region but are constant below about 100m depth at 2400m/s. Model Q-factors for the constant velocity depth region below about 100m are also assumed to be constant at  $Q = 150$ . An empirical equation of Waters (1978) is utilized to compute P-wave Q-factors from P-wave velocities in the near-field region above 100m depth according to

$$Q_{z-\Delta z} = Q_z \left[ \frac{v_{z-\Delta z}}{v_z} \right]^2. \quad (4)$$

Q-factors computed with Equation 4 for the near-field velocity model of Figure 8 are plotted in Figures 9 and 10 for comparison purposes.

When the spectral ratio method of Q-estimation is applied to VSP-traces computed with a multi-interface Sommerfeld integral (Haase, 2008) for the velocity step model introduced above, the Q-factors displayed in Figure 9 are obtained. Model Q-factors are clearly not recovered. In comparing the model result of Figure 9 to real-data spectral ratio method Q-estimates shown in Figure 6 a similarity in multi *wrap-around* behavior is observed. As noted previously, the spectral ratio method is a far-field method and, depending on relative near-field strength, significant estimation errors can be present. A spectral compensation approach for homogeneous near-fields (Haase and Stewart, 2008) does not work for this inhomogeneous situation. The same multi-interface Sommerfeld integral that is used to generate VSP-traces for the above stepped velocity model is used next to recover Q-factors by inversion.

### Q-ESTIMATION FOR THE INHOMOGENEOUS NEAR-FIELD MODEL

From using the Sommerfeld integral to compute VSP-traces for a 1D-earth model, it is only a short step to an inversion algorithm for Q-factors when the assumption is made that velocities and densities are known. According to Cheriff's Encyclopedic Dictionary, *inversion* means

*“deriving from field data a model to describe the subsurface that is consistent with the data”.*

*Field data* in this situation means the VSP-traces generated from the velocity/density/Q model. Q-factors are the only unknowns when velocities and densities are assumed to be given. For every depth step, forward model VSP-traces are computed with Q-factors in the range from 10 to 150 as a first attempt to find  $Q(z)$ . The presumed correct answer is determined by the least square difference between data and forward model at every depth and plotted in Figure 10. Even though far from ideal, this first attempt is a substantial improvement when compared to the spectral ratio equivalent in Figure 9. Squared differences are computed in the frequency domain, one frequency point at a time for a predetermined bandwidth, by summing the squared differences of the real parts and the imaginary parts. Figure 11 shows the result of an exhaustive search at two adjacent depth levels across the first (shallowest) velocity step. Clearly, the correct model Q at the minimum location could be recovered in this ideal model situation but at considerable computational cost. *Parabolic* assumptions are valid only in the immediate vicinity of the minimum and the challenge in this situation is to find a starting point within this *parabolic* range. When the differences between data and model are summed directly (without squaring) and separately for real and imaginary parts of the corresponding frequency points the curves in Figure 12 result. The sums of the real parts and of the imaginary parts of the differences are zero when the trial Q approximately equals the model Q. Departures are caused by the assumption of effective Q-factors below the current layer. For the computation of the black curves in Figure 12 the current layer is at  $z = 44\text{m}$  depth and for all layers deeper than 44m  $Q = 100$  is assumed; the blue curves at  $z = 42\text{m}$  are exact because there are no discontinuities shallower than 44m and the down-going wave at  $z = 42\text{m}$  is undisturbed in this model situation. The advantage of the *hyperbolas* in Figure 12 lies in the fact that, with only three function evaluations, curves can be fitted and initial Q-estimates obtained. The coefficients of

$$y = a + \frac{b}{x} + c/x^2 \quad (5)$$

are determined from the sums computed at trial Q-factors of 10, 40 and 160 (separately for real parts and then imaginary parts) and the initial Q-estimates are calculated from Equation 5 by setting  $y = 0$  and  $x = Q_z$  giving

$$Q_{z1,z2} = -\frac{b}{2a} \pm \sqrt{\left(\frac{b}{2a}\right)^2 - \frac{c}{a}} \quad (6)$$

The average of  $Q_{z\text{-real}}$  and  $Q_{z\text{-imaginary}}$  is used as input for the next iteration. Assuming that

$$Q_{\text{init}} = (Q_{z\text{-re}} + Q_{z\text{-im}})/2 \quad (7)$$

is within *parabolic* range of the true minimum we make two more function evaluations at  $Q_{\text{init}}-\Delta Q$  and  $Q_{\text{init}}+\Delta Q$  with  $\Delta Q$  set to 0.1 and determine the minimum of the *parabola*; only if the summed squares at  $Q_{\text{init}}-\Delta Q$  and  $Q_{\text{init}}+\Delta Q$  are at least moderately asymmetric do we make a second *parabolic* pass to find the optimum Q. Figure 13 compares  $Q_{\text{init}}$  as obtained from the *hyperbolic* pass and  $Q_{\text{optimum}}$  as obtained from the *parabolic* pass (or passes) to the original model Q. The Q-estimation error of the *hyperbolic* fit is seen to increase with depth but the remaining error after additional *parabolic* correction is sufficiently small even for this model situation of stepped velocities.

## CONCLUSIONS

Based on near-field multiplier normalized spectral ratios it is shown that locations in depth of large negative and positive spectral ratio method Q-estimates with *wrap-around* appearance are controlled by P-wave velocities and intrinsic Q-factors; *wrap-around* depths increase with velocity increases and also with intrinsic Q-factor increases.

A velocity-step model is introduced to provide multiple *wrap-around* points and test Q-recovery techniques. We show that model Q-factors can be recovered exactly when both, VSP model data and an exhaustive-Q-search forward model are generated with the same multi interface Sommerfeld integral and assuming all velocities as well as densities (but not Q-factors) are known for the forward modelling step. In this approach we are seeking to minimize the sum of squared differences between data and forward model. Computational efficiencies can be gained by hyperbolic fitting of the sum of differences (without squaring) to obtain an initial guess for the Q-factor as a function of depth that is within parabolic range of the sum of squared differences minimum. Results for a real data situation are expected to be less than perfect because, firstly, velocities and densities are not exactly known and, secondly, field data is noise contaminated.

## ACKNOWLEDGEMENTS

Support from the CREWES Project at the University of Calgary and its industrial sponsorship is gratefully acknowledged.

## REFERENCES

- Haase, A.B., 2008, Extending Sommerfeld integral based spherical wave field computations beyond two layers: CREWES Research Report, Volume 20
- Haase, A.B., and Stewart, R.R., 2008, Modeling near-field effects in VSP-based Q-estimation: CREWES Research Report, Volume 20
- Ortiz-Osornio, M., and Schmitt, D., 2008, Q Inversion in a Heavy Oil Sand: Annual CSEG Meeting (2008 C3GEO Convention), Expanded Abstracts, 489-492.
- Waters, K.H., 1978, Reflection Seismology: John Wiley and Sons, Inc., page 203.

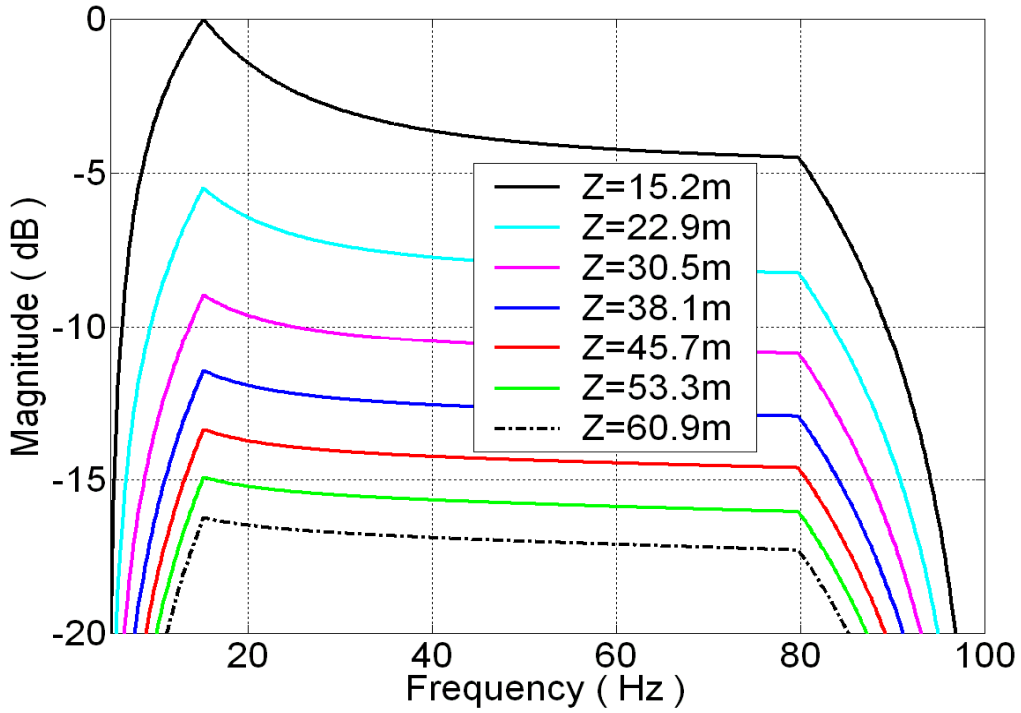


FIG.1. Near-field log-magnitude spectra for the depth range from 15 m to 61 m computed with a Sommerfeld-integral algorithm (global scaling to zero dB with relative amplitudes retained).

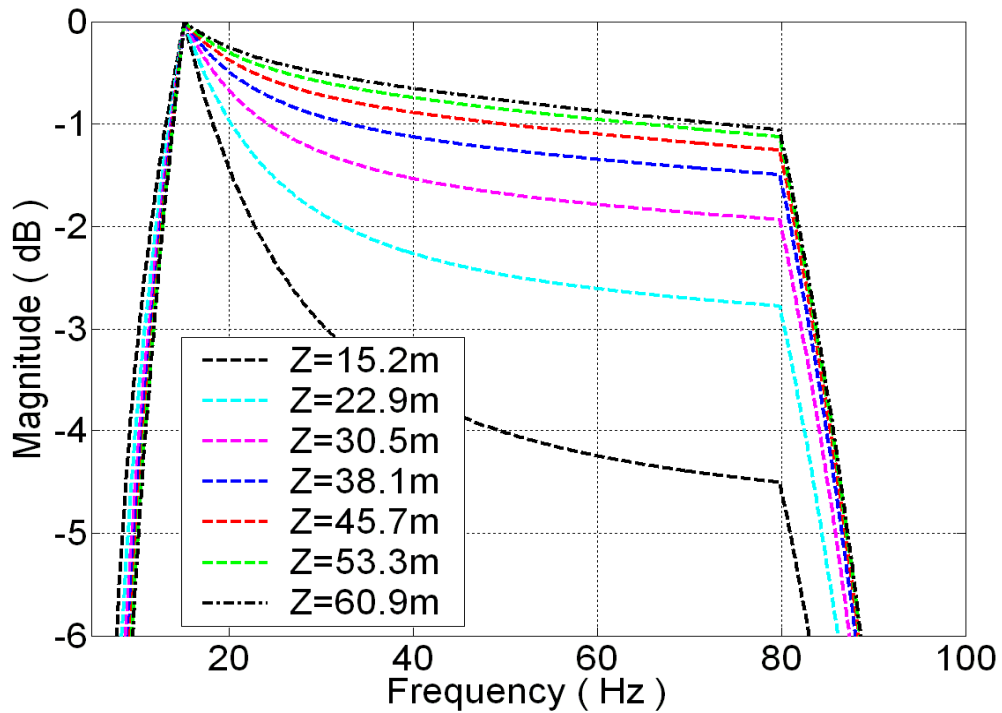


FIG.2. Near-field log-magnitude spectra with all spectra equalized to their maximum amplitudes (zero dB scaling applied individually. The down going wave appears to gain high frequency strength. Note the vertical scale differs from Figure 1.

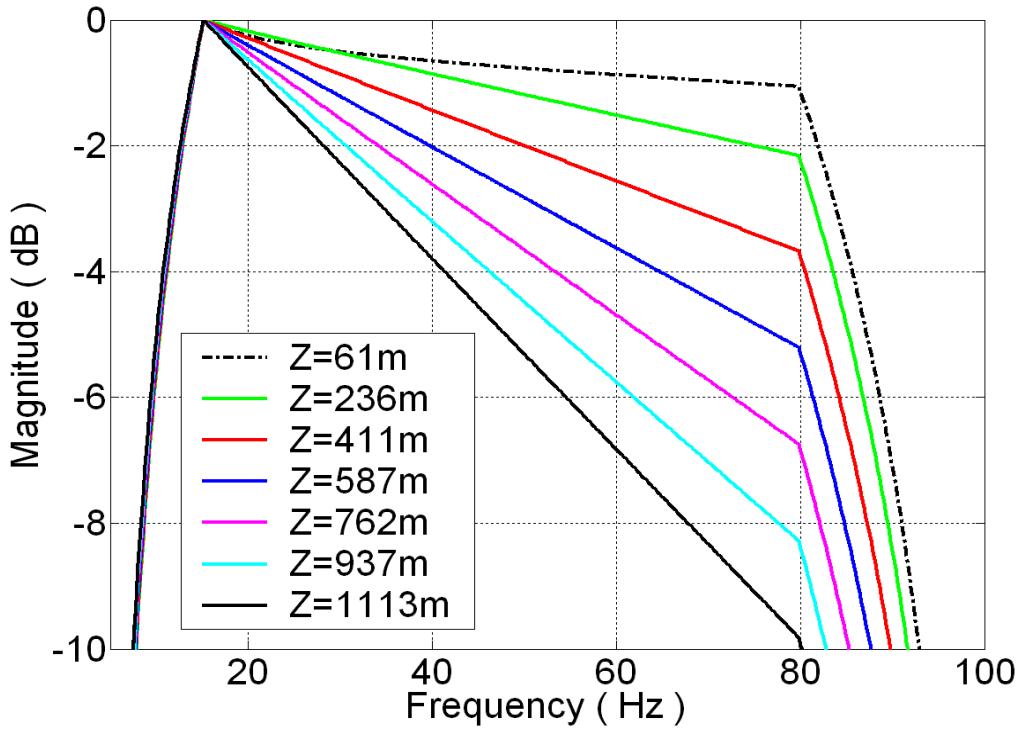


FIG.3. Far-field log-magnitude spectra with zero dB scaling applied individually.

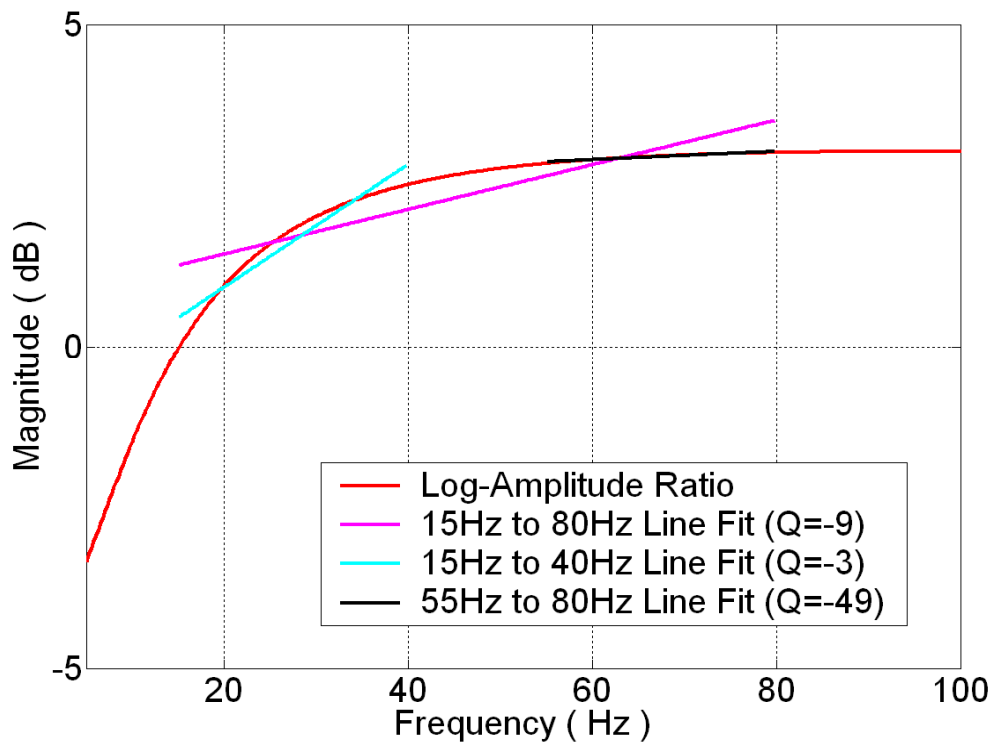


FIG.4. Straight line fit to log spectral ratios between depth levels 15m and 38m.

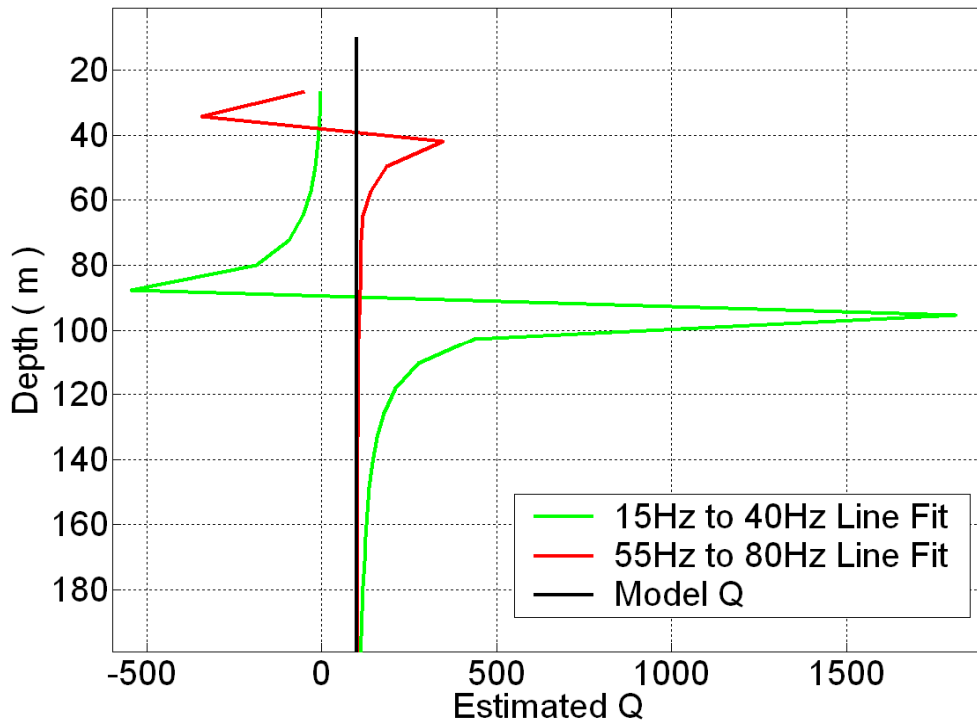


FIG.5. Apparent near-field frequency dependence of Q. Note the polarity change of Q.

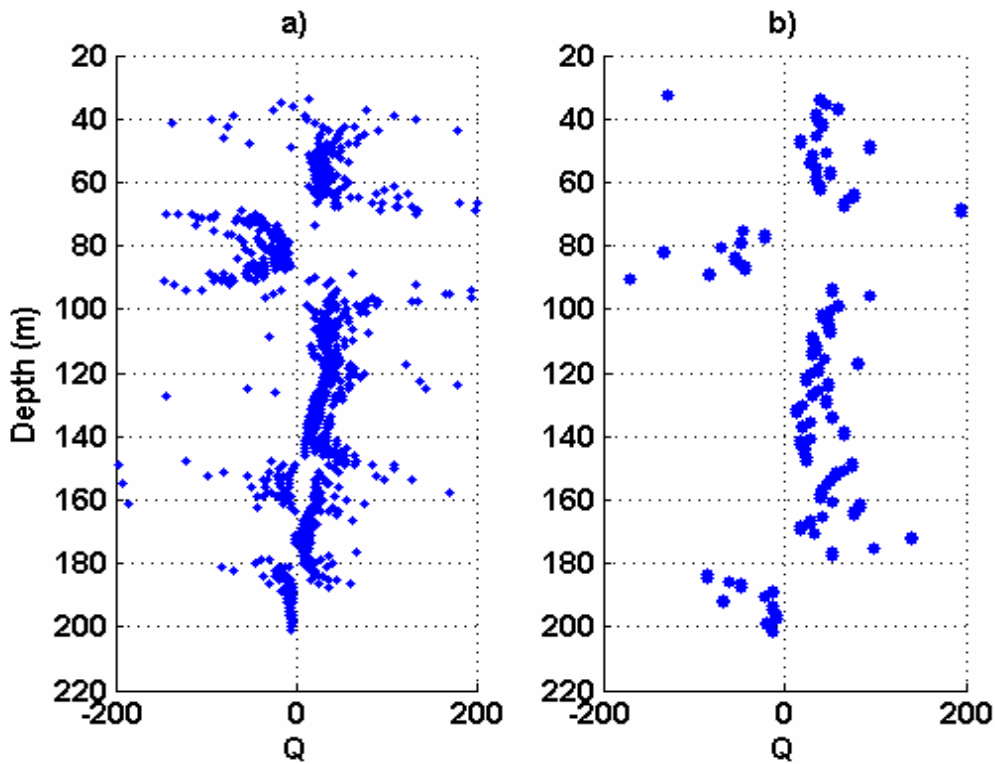


FIG.6. Heavy oil sand Q-factors [Ortiz-Osornio and Schmitt, 2008: a) the traditional spectral ratio technique, and b) their inversion algorithm].

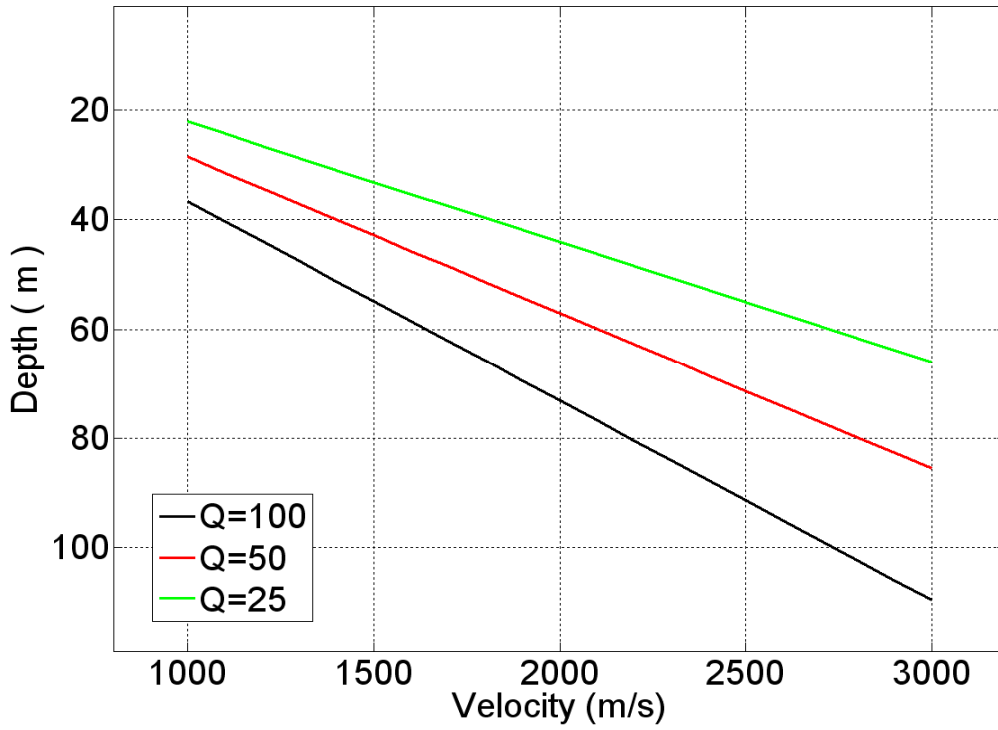


FIG.7. Wrap-around depth as function of velocity and Q-factor.

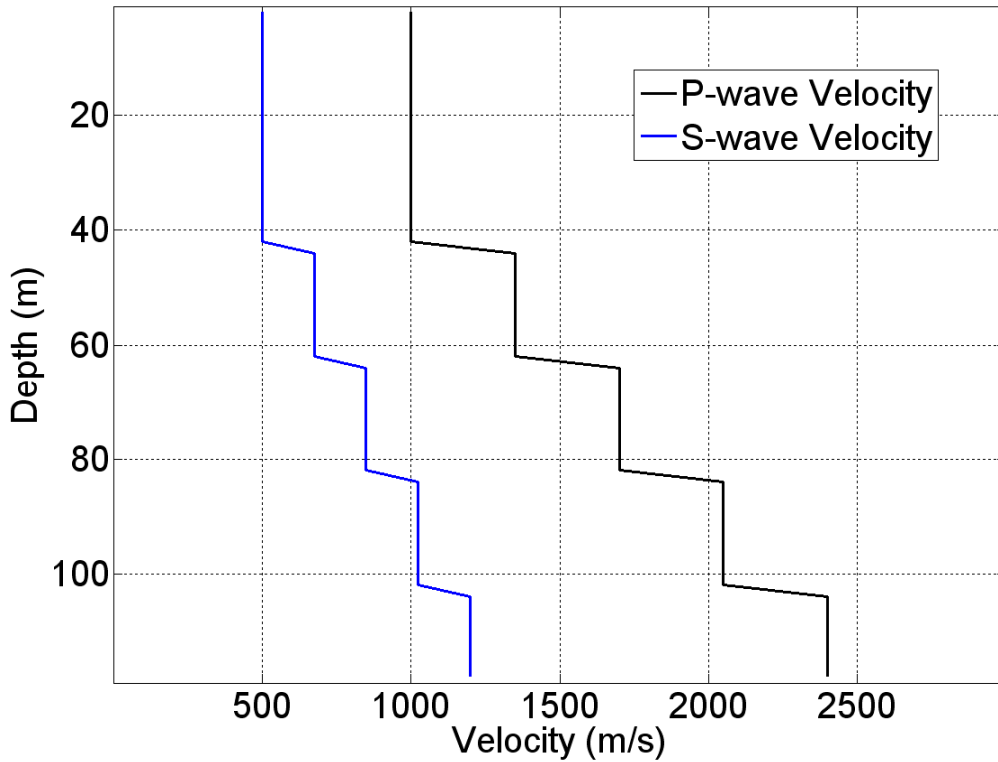


FIG.8.  $V_p$  and  $V_s$  versus depth for stepped-velocity near-field VSP model.

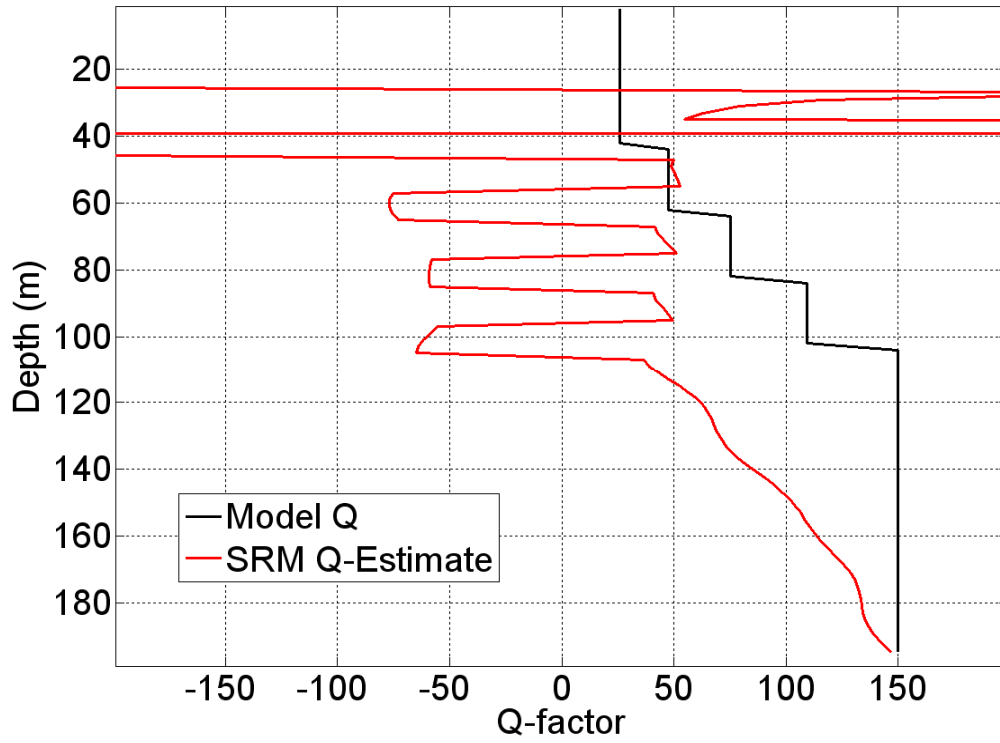


FIG.9. Spectral ratio method (SRM) Q-estimate compared to stepped velocity model Q.

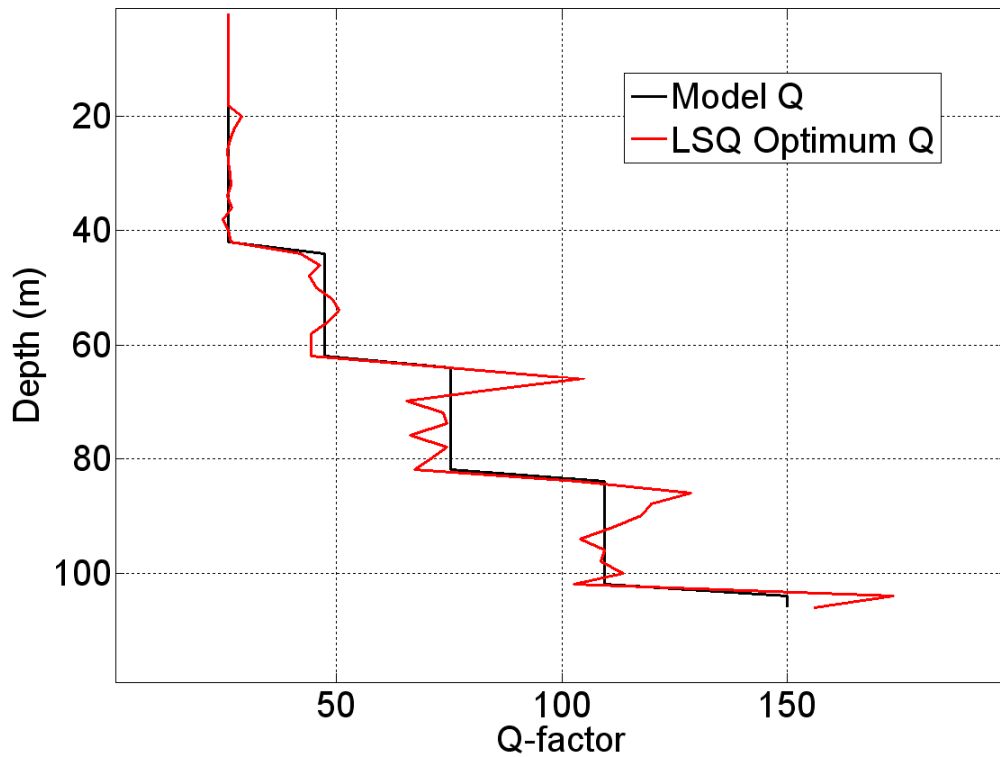


FIG.10. Inversion Q-estimate compared to stepped velocity model Q.

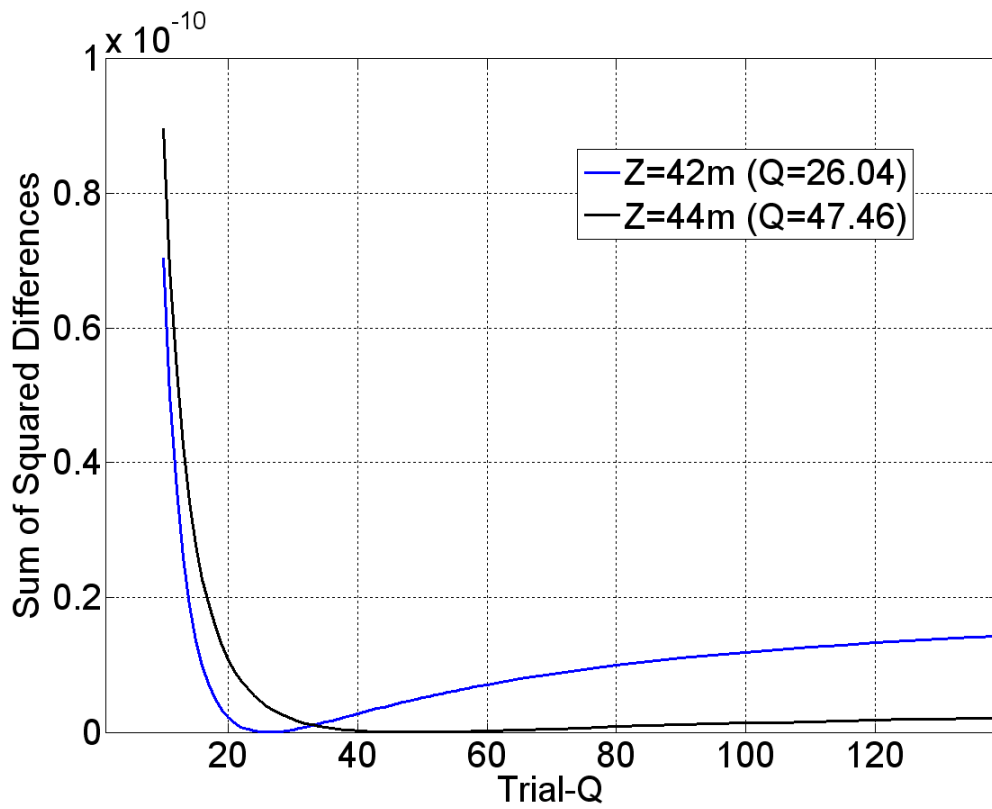


FIG.11a. Sum of squared differences between data and forward model (linear scale).

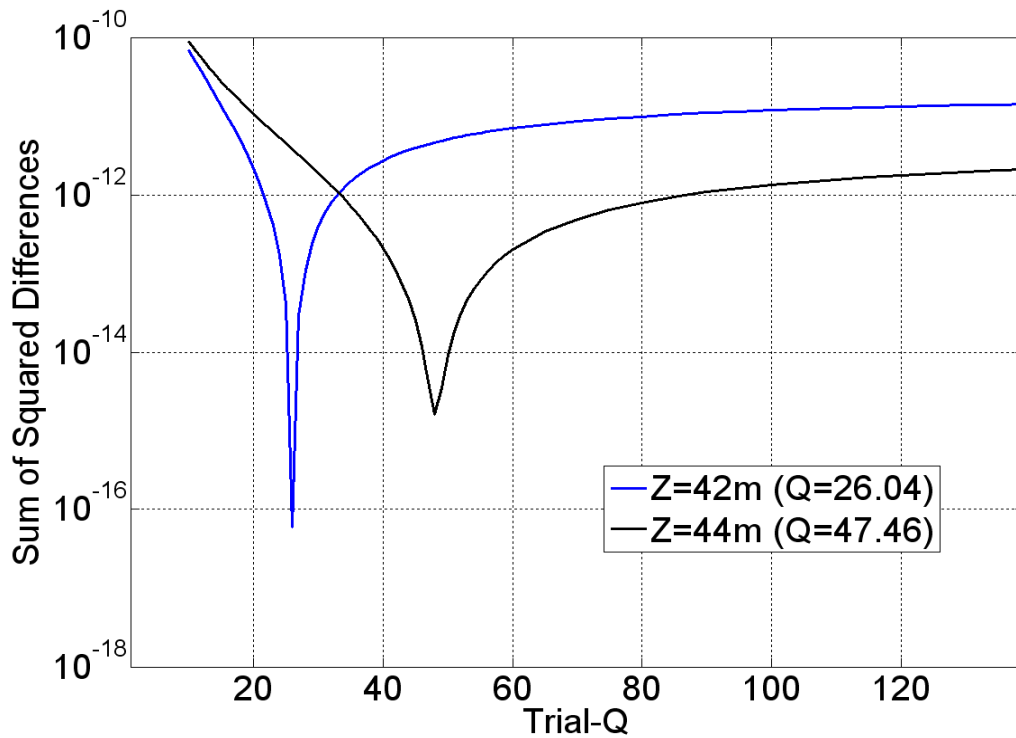


FIG.11b. Sum of squared differences between data and forward model (log scale).

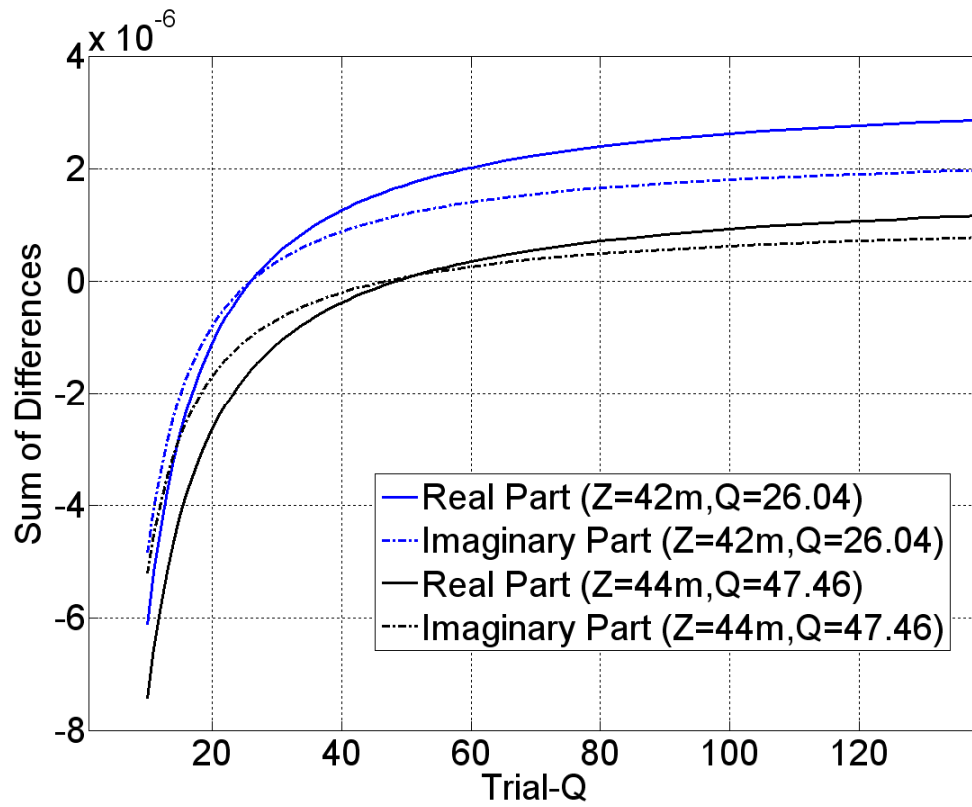


FIG.12. Sum of differences between data and forward model.

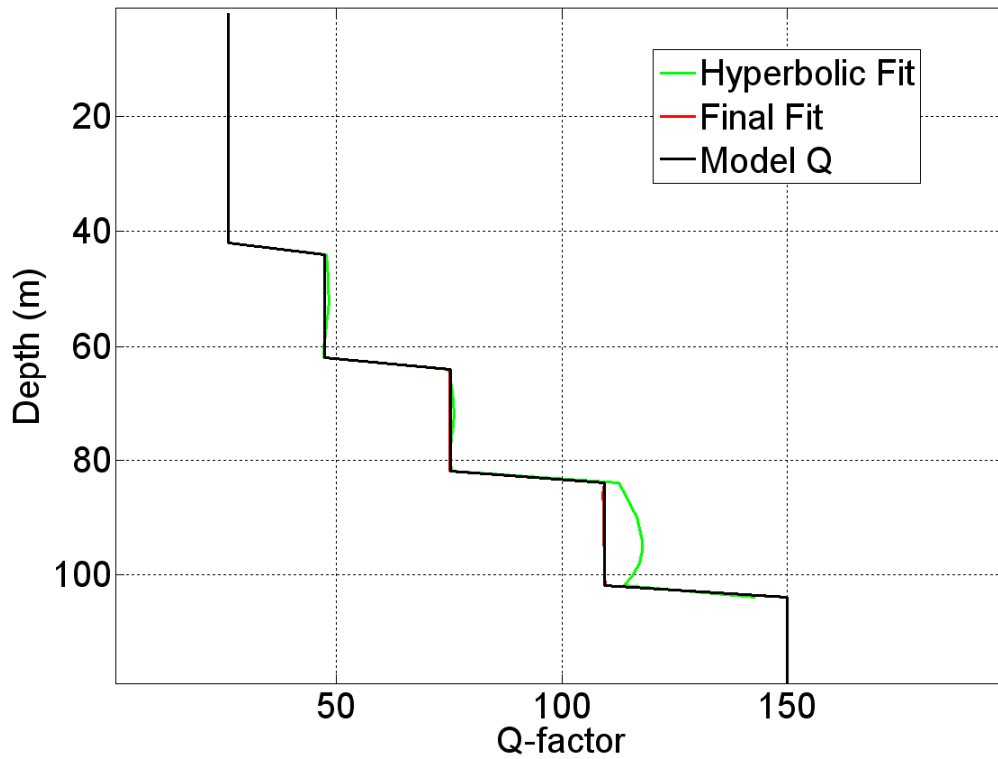


FIG.13. Q versus depth for stepped-velocity near-field VSP model.